RÉPUBLIQUE FRANÇAISE
Liberté
Égalité
Fraternité

Robust Statistics for Multi-Band SAR Image Change Detection

EUSIPCO, Lyon 2024

Moustapha Diaw[1], Olivier Lerda[3], Joana Frontera-Pons[1], Frédéric Brigui[1] and Jean-Philippe Ovarlez[1, 2]

[1]ONERA DEMR, [2]CentraleSupélec, SONDRA [3]Exail Sonar Systems Division

Plan

- Introduction
  - Background on change detection methods in SAR imagery
  - Problems in multivariate and multiband SAR image analysis.
  - Contributions in multiband SAR image change detection
- Proposed multiband change detection method
  - Multiband SAR modeling
  - Derivation of the detector
  - Applications
    - Simulated data - False Alarm Regulation
    - Simulated data - Probability of Detection (PD) vs Signal-to-Noise -Ratio (SNR)
    - Real data - L and X bands SETHI polarimetric SAR images.
- Conclusions and future works

Introduction

Background- Detection concept for polarimetric SAR image [1]

- Mono-band

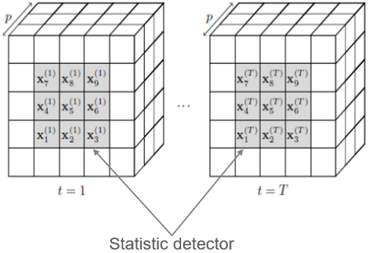

- Multiband

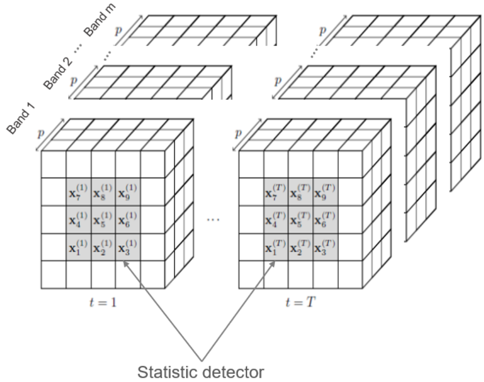

In our case $T = 2$, $\mathbf{x}_5^{(t)}$ is the test pixel at time t.

Introduction

Background - Conventional Conradsen's detector [2] on single-band

The vector $\mathbf{x} \in \mathbb{C}^p$ is distributed according to complex circular Normal $\mathcal{CN}\left(\mathbf{0}_p, \mathbf{\Phi}\right)$ distribution to handle spatial SAR image homogeneity:

$$p_{\mathbf{x}}(\mathbf{x}, \mathbf{\Phi}) = \frac{1}{\pi^p \left|\mathbf{\Phi}\right|} \exp\left(-\mathbf{x}^H \mathbf{\Phi}^{-1} \mathbf{x}\right),$$

where $\mathbf{\Phi}$ is the unknown covariance matrix.

Detection problem: $\begin{cases} H_0 : \mathbf{\Phi}_1 = \mathbf{\Phi}_2 \\ H_1 : \mathbf{\Phi}_1 \neq \mathbf{\Phi}_2 \end{cases}$

The Conradsen's classical Gaussian detector [2] is given by:

$$\hat{\Lambda}_G = \frac{\left|\hat{\mathbf{\Phi}}^{SCM}\right|^{2N}}{\prod_{t=1}^{t=2} \left|\hat{\mathbf{\Phi}}_t^{SCM}\right|^{N}} \underset{H_0}{\overset{H_1}{\gtrless}} \lambda,$$

where $\hat{\mathbf{\Phi}}^{SCM}$ and $\hat{\mathbf{\Phi}}_t^{SCM}$ are Sample Covariance Matrices.

Introduction

Background - A. Mian Detector [1] on single-band

The vector $\mathbf{x} \in \mathbb{C}^p$ is distributed according to $\mathcal{CN}\left(\mathbf{0}_p, \tau\, \mathbf{\Phi}\right)$ to handle spatial SAR image heterogeneity.

$$p_{\mathbf{x}}(\mathbf{x}, \mathbf{\Phi}) = \frac{1}{\pi^p\, \tau^p\, \left|\mathbf{\Phi}\right|} \exp\left(-\frac{\mathbf{x}^H\, \mathbf{\Phi}^{-1}\, \mathbf{x}}{\tau}\right),$$

where the covariance matrix $\mathbf{\Phi}$ and the positive scalar texture τ are unknown parameters.

Detection problem: $\begin{cases} H_0 : \{\mathbf{\Phi}_1, \tau_1\} = \{\mathbf{\Phi}_2, \tau_2\} \\ H_1 : \{\mathbf{\Phi}_1, \tau_1\} \neq \{\mathbf{\Phi}_2, \tau_2\} \end{cases}$

The Mian's GLRT Detector [1] is defined as:

$$\hat{\Lambda}_{MT} = \frac{\left|\hat{\mathbf{\Phi}}^{FP}\right|^{2N}}{\prod\limits_{t=1}^{t=2}\left|\hat{\mathbf{\Phi}}_t^{FP}\right|^{N}} \prod_{k=1}^{k=N} \frac{\left|\hat{\tau}_k\right|^4}{\prod\limits_{t=1}^{t=2}\left|\hat{\tau}_k^t\right|^2} \underset{H_0}{\overset{H_1}{\gtrless}} \lambda,$$

where $\hat{\mathbf{\Phi}}^{FP}$ and $\hat{\mathbf{\Phi}}_t^{FP}$ are Tyler Covariance Matrices.

Introduction

Problems and Contributions

Identified problems for multi-band case:

- Textures (or heterogeneity) are not taken into account in the design of the Gaussian detector $\hat{\Lambda}_G$.
- The detector $\hat{\Lambda}_{MT}$ will perform better only if the concatenated bands are characterized by the same texture.

Contributions:

- Proposal for a multi-band change detection detector that considers heterogeneous nature and variations in texture across the merged bands (inspired by [3]).
- Applications on simulated data to analyse regulation of False Alarm and performance in terms of PD/SNR.
- Applications on polarimetric SAR data simultaneously acquired at two bands, L and X, by the ONERA SETHI SAR system at two different dates, t_1 and t_2 at Captieux.

Proposed multiband change detection method

Multiband SAR modeling

The vector $\mathbf{x} = \left[\mathbf{x}_1^T, \mathbf{x}_2^T, \ldots, \mathbf{x}_m^T\right]^T \in \mathbb{C}^{mp}$ is distributed as $\mathcal{CN}\left(\mathbf{0}_{m\,p}, \boldsymbol{\Sigma}\right)$:

$$p_{\mathbf{x}}(\mathbf{x}) = \frac{1}{\pi^{m\,p}\left|\boldsymbol{\Sigma}\right|} \exp\left(-\mathbf{x}^H \boldsymbol{\Sigma}^{-1} \mathbf{x}\right),$$

where $\mathbf{x}_i = \sqrt{\tau_i}\, \mathbf{z}_i$ and with $\boldsymbol{\Sigma} = E\left(\mathbf{x}\,\mathbf{x}^H\right) = \mathbf{T}\,\boldsymbol{\Phi}\,\mathbf{T}$ where

$$\boldsymbol{\Phi} = \begin{pmatrix} E\left(\mathbf{z}_1\mathbf{z}_1^H\right) & E\left(\mathbf{z}_1\mathbf{z}_2^H\right) & \ldots & E\left(\mathbf{z}_1\mathbf{z}_m^H\right) \\ E\left(\mathbf{z}_2\mathbf{z}_1^H\right) & E\left(\mathbf{z}_2\mathbf{z}_2^H\right) & \ldots & E\left(\mathbf{z}_2\mathbf{x}_m^H\right) \\ \vdots & \vdots & \ddots & \vdots \\ E\left(\mathbf{z}_m\mathbf{z}_1^H\right) & E\left(\mathbf{z}_m\mathbf{z}_2^H\right) & \ldots & E\left(\mathbf{z}_m\mathbf{z}_m^H\right) \end{pmatrix}, \quad \mathbf{T} = \begin{pmatrix} \sqrt{\tau_1}\,\mathbf{I}_p & \mathbf{0}_p & \ldots & \mathbf{0}_p \\ \mathbf{0}_p & \sqrt{\tau_2}\,\mathbf{I}_p & \ldots & \mathbf{0}_p \\ \vdots & \vdots & \ddots & \vdots \\ \mathbf{0}_p & \mathbf{0}_p & \ldots & \sqrt{\tau_m}\,\mathbf{I}_p \end{pmatrix}.$$

The change detection problem is then characterized by: $\begin{cases} H_0 : \boldsymbol{\Sigma}_1 = \boldsymbol{\Sigma}_2 \\ H_1 : \boldsymbol{\Sigma}_1 \neq \boldsymbol{\Sigma}_2 \end{cases}.$

Proposed multiband change detection method

Derivation of the detector - Estimation by the joint fixed-point method

The parameters $\left(\hat{\mathbf{\Phi}}, \left\{\hat{\mathbf{T}}_k\right\}_{k\in\{1,N\}}\right)$ et $\left(\left\{\hat{\mathbf{T}}_k^t\right\}_{k\in\{1,N\},t\in\{1,2\}}, \left\{\hat{\mathbf{\Phi}}^t\right\}_{t\in\{1,2\}}\right)$ are given:

- by the two following joint fixed point equations under H_0,

$$\begin{cases} \hat{\mathbf{T}}_k = \frac{1}{2}\sum_{t=1}^{2} \mathrm{Re}\left(\hat{\mathbf{\Phi}}^{-1}\hat{\mathbf{T}}_k^{-1}\,\mathbf{x}_k^t\,\mathbf{x}_k^{tH}\right), \quad \forall k \in \{1, N\}, \\ \hat{\mathbf{\Phi}} = \frac{1}{2N}\sum_{k=1,t=1}^{k=N,\,t=2} \hat{\mathbf{T}}_k^{-1}\,\mathbf{x}_k^t\,\mathbf{x}_k^{tH}\,\hat{\mathbf{T}}_k^{-1}. \end{cases}$$

- and by the two following joint fixed point equations under H_1,

$$\begin{cases} \hat{\mathbf{T}}_k^t = \mathrm{Re}\left(\hat{\mathbf{\Phi}}_t^{-1}\left(\hat{\mathbf{T}}_k^t\right)^{-1}\mathbf{x}_k^t\,\mathbf{x}_k^{tH}\right), \quad \forall k \in \{1, N\}, \forall t \in \{1, 2\} \\ \hat{\mathbf{\Phi}}_t = \frac{1}{N}\sum_{k=1}^{N}\left(\hat{\mathbf{T}}_k^t\right)^{-1}\mathbf{x}_k^t\,\mathbf{x}_k^{tH}\left(\hat{\mathbf{T}}_k^t\right)^{-1}, \quad \forall t \in \{1, 2\} \end{cases}$$

Proposed multiband change detection method

Derivation of the detector

Estimating the parameters $(\mathbf{T}_k, \mathbf{\Phi})$ under H_0 and $(\mathbf{T}_k^t, \mathbf{\Phi}_t)$ under H_1 with N secondary data through Generalized Maximum Likelihood Estimation procedure leads to:

$$\hat{\Lambda}_B = \frac{\left|\hat{\mathbf{\Phi}}\right|^{2N}}{\prod_{t=1}^{2}\left|\hat{\mathbf{\Phi}}_t\right|^{N}} \prod_{k=1}^{N} \frac{\left|\hat{\mathbf{T}}_k\right|^{4}}{\prod_{t=1}^{2}\left|\hat{\mathbf{T}}_k^t\right|^{2}} \underset{H_0}{\overset{H_1}{\gtrless}} \lambda\,,$$

where λ is the detection threshold.

Recall: *CFAR (Constant False Alarm Regulation) Matrix or Texture property* means independence of the detection test with the PDF parameters!

Results

Simulated data - False Alarm Regulation

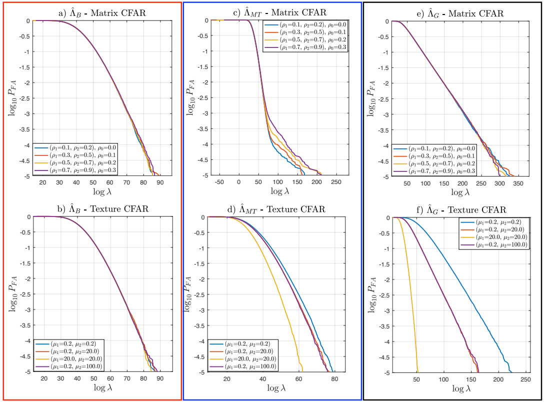

Proposed Method | Mian's Method | Conradsen's Method

P_{FA} vs λ with $N = 16$, $p = 3$, $m = 2$, $k = 1$.

- $\mathbf{x} = \left(\mathbf{x}_1^T, \mathbf{x}_2^T\right)^T$, $\boldsymbol{\mathcal{T}}(\rho) = \left(\rho^{|i-j|}\right)_{i,j}$
- Band 1: $\boxed{\mathbf{x}_1 = \sqrt{\tau_1}\,\mathbf{z}_1}$

  where $\begin{cases} \mathbf{z}_1 \sim \mathcal{CN}(\mathbf{0}_p, \boldsymbol{\mathcal{T}}(\rho_1)) \\ \tau_1 \sim \Gamma(\mu_1, 1/\mu_1) \end{cases}$.
- Band 2: $\boxed{\mathbf{x}_2 = \sqrt{\tau_2}\,\mathbf{z}_2}$

  where $\begin{cases} \mathbf{z}_2 \sim \mathcal{CN}(\mathbf{0}_p, \boldsymbol{\mathcal{T}}(\rho_2)) \\ \tau_2 \sim \Gamma(\mu_2, k/\mu_2) \\ k \in \mathbb{R}^+ \text{ scale factor.} \end{cases}$.
- Interband: $E\left(\mathbf{z}_1\,\mathbf{z}_2^H\right) = \rho_0\,\mathbf{1}_p$.

Results

Simulated data - Probability of Detection vs SNR (in dB)

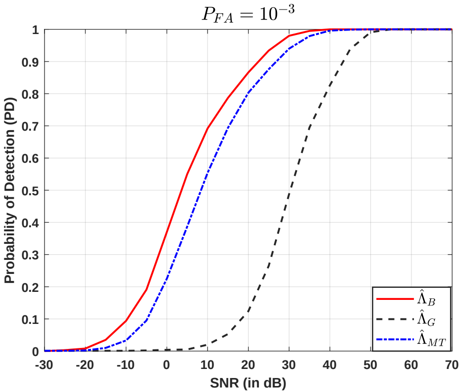

Probability of detection vs SNR with textured Gaussian simulated data over two frequency bands ($\rho_1 = 0.1$, $\rho_2 = 0.5$, $\rho_0 = 0.1$, $\mu_1 = 1$ and $\mu_2 = 0.1$, with scale factor $k = 50$ for $P_{FA} = 10^{-3}$.

At PD = 0.7, $\hat{\Lambda}_B$ gains approximately 5 and 25 dB compared to $\hat{\Lambda}_{MT}$ and $\hat{\Lambda}_G$, respectively.

Real data

L and X band SETHI POLSAR images in Pauli basis in RGB color composition

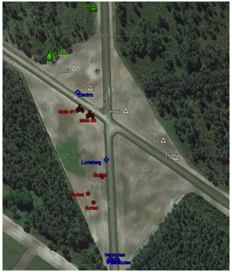

Ground truth of the studied scene

L-band - t_1

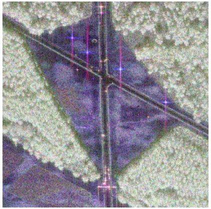

X-band - t_1

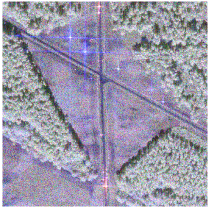

L-band - t_2

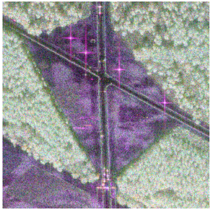

X-band - t_2

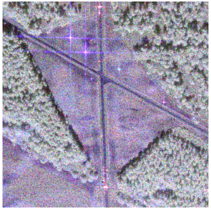

Results on experimental SETHI data

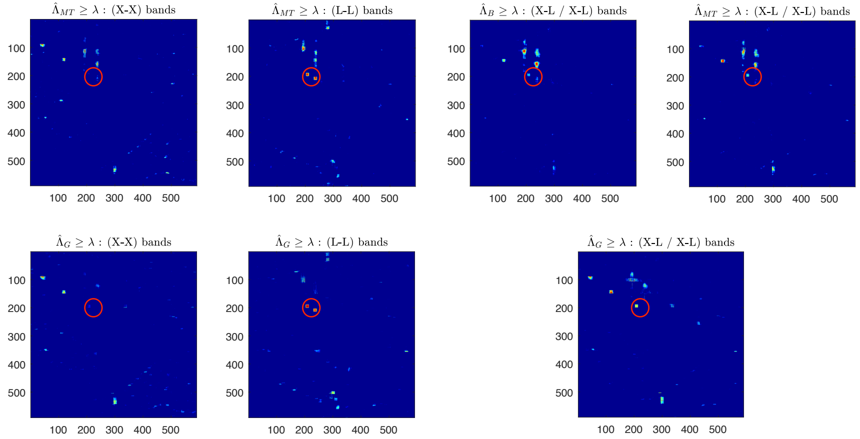

Left: Mono-band detectors $\hat{\Lambda}_{MT}$ and $\hat{\Lambda}_{G}$. **Right:** L-X multi-band detectors $\hat{\Lambda}_{MT}$, $\hat{\Lambda}_{G}$ and $\hat{\Lambda}_{B}$ ($P_{fa} = 10^{-3}$).

Conclusions and future works

In this work, we have,

- proposed a robust statistic for multi-band SAR image change detection and analyzed his performance,
- applied the proposed detector on simulated data and SETHI SAR images in L and X bands at two dates t_1 and t_2,
  - the proposed detector are CFAR with respect to matrix and texture,
  - the proposed detector outperforms the state-of-the-art methods in terms of PD vs SNR and in terms of PFA regulation.
  - it shows promising results on real data when combining X-band and L-band.

In the future works, we will,

- analyze the convergence of the joint fixed point equations,
- analyze the performance on experimental data of the proposed detector on more than two bands.

References

[1] A. Mian, G. Ginolhac, J.-P. Ovarlez, and A. M. Atto, “New robust statistics for change detection in time series of multivariate SAR images,” *IEEE Transactions on Signal Processing*, vol. 67, no. 2, pp. 520–534, 2019.

[2] K. Conradsen, A. A. Nielsen, J. Schou, and H. Skriver, “Change detection in polarimetric SAR data and the complex Wishart distribution,” in *IGARSS 2001. Scanning the Present and Resolving the Future. Proceedings. IEEE 2001 International Geoscience and Remote Sensing Symposium (Cat. No.01CH37217)*, vol. 6, pp. 2628–2630 vol.6, 2001.

[3] O. Lerda, A. Mian, G. Ginolhac, J.-P. Ovarlez, and D. Charlot, “Robust Detection for Mills Cross Sonar,” *IEEE Journal of Oceanic Engineering*, vol. 49, no. 3, pp. 1009–1024, 2024.

Thank you for your attention!

Any questions?

Appendix

Maximum Likelihood Estimation procedure with N secondary data to derive the detector:

$$\Lambda_B(\mathbf{x}) = \frac{\mathcal{L}_1\left(\left\{\left\{\mathbf{x}_k^t, \mathbf{T}_k^t\right\}_{k\in[1,N]}, \mathbf{\Phi}_t\right\}_{t\in[1,2]}\right)}{\mathcal{L}_0\left(\left\{\left\{\mathbf{x}_k^t\right\}_{k\in[1,N]}\right\}_{t\in[1,2]}, \left\{\mathbf{T}_k\right\}_{k\in[1,N]}, \mathbf{\Phi}\right)},$$

$$\mathcal{L}_1\left(\left\{\left\{\mathbf{x}_k^t, \mathbf{T}_k^t\right\}_k, \mathbf{\Phi}_t\right\}_t\right) = \prod_{\substack{k=1\\t=1}}^{\substack{k=N\\t=2}} p_{\mathbf{x}}\left(\mathbf{x}_k^t, \mathbf{T}_k^t \mathbf{\Phi}_t \mathbf{T}_k^t\right),$$

$$\mathcal{L}_0\left(\left\{\left\{\mathbf{x}_k^t\right\}_k\right\}_t, \left\{\mathbf{T}_k\right\}_k, \mathbf{\Phi}\right) = \prod_{\substack{k=1\\t=1}}^{\substack{k=N\\t=2}} p_{\mathbf{x}}\left(\mathbf{x}_k^t, \mathbf{T}_k \mathbf{\Phi} \mathbf{T}_k\right).$$

To maximize the two likelihood functions, $\mathcal{L}0$ and $\mathcal{L}1$, we need to perform the following ope

Appendix

To maximize the two likelihood functions, $\mathcal{L}0$ and $\mathcal{L}1$, we need to perform the following operations: By denoting $C = -2\, m\, p\, N\, \log(\pi)$, the logarithm of (15), under H_0, is given by:

$$\log(\mathcal{L}_0) = C - \sum_{\substack{k=1\\t=1}}^{\substack{k=N\\t=2}} \log\left(|\mathbf{\Phi}|\right) + 2\sum_{\substack{k=1\\t=1}}^{\substack{k=N\\t=2}} \log\left(\left|\mathbf{T}_k^{-1}\right|\right) - \sum_{\substack{k=1\\t=1}}^{\substack{k=N\\t=2}} \left(\mathbf{x}_k^{tH}\,\mathbf{T}_k^{-1}\mathbf{\Phi}^{-1}\mathbf{T}_k^{-1}\,\mathbf{x}_k^t\right)\;.$$

Now, we proceed by taking the derivative with respect to $\mathbf{T}_k^{-1}$. Then, $\forall k \in [1, N]$,

$$\frac{\partial \log(\mathcal{L}_0)}{\partial \mathbf{T}_k^{-1}} = 4\sum_{k=1}^{k=N} \mathbf{T}_k - 2\sum_{\substack{k=1\\t=1}}^{\substack{k=N\\t=2}} \mathrm{Re}\left((\mathbf{\Phi}\mathbf{T}_k)^{-1}\mathbf{x}_k^t\mathbf{x}_k^{tH}\right) = \mathbf{0}_{m\,p}\,.$$

Appendix

As $\dfrac{\partial \log\left(\left|\mathbf{T}_k^{-1}\right|\right)}{\partial \mathbf{T}_k^{-1}} = \mathbf{T}_k$ and $\mathbf{x}_k^{tH}\left(\mathbf{T}_k \boldsymbol{\Phi} \mathbf{T}_k\right)^{-1}\mathbf{x}_k^t$ is a positive real scalar, then,

$$\mathbf{x}_k^{tH}\left(\mathbf{T}_k \boldsymbol{\Phi} \mathbf{T}_k\right)^{-1}\mathbf{x}_k^t = \mathrm{Re}\left(\mathrm{tr}\left(\mathbf{T}_k^{-1}\boldsymbol{\Phi}^{-1}\mathbf{T}_k^{-1}\,\mathbf{x}_k^t\,\mathbf{x}_k^{tH}\right)\right) .$$

we obtain,

$$\frac{\partial \mathrm{tr}\left(\mathbf{T}_k^{-1}\boldsymbol{\Phi}^{-1}\mathbf{T}_k^{-1}\,\mathbf{x}_k^t\,\mathbf{x}_k^{tH}\right)}{\partial \mathbf{T}_k^{-1}} = 2\,\mathrm{Re}\left(\boldsymbol{\Phi}^{-1}\,\mathbf{T}_k^{-1}\,\mathbf{x}_k^t\,\mathbf{x}_k^{tH}\right) .$$

Optimizing each $\hat{\mathbf{T}}_k$ individually results in:

$$\forall k \in [1, N], \hat{\mathbf{T}}_k = \frac{1}{2}\sum_{t=1}^{t=2} \mathrm{Re}\left(\boldsymbol{\Phi}^{-1}\hat{\mathbf{T}}_k^{-1}\mathbf{x}_k^t\mathbf{x}_k^{tH}\right) .$$

Appendix

Let us estimate $\mathbf{\Phi}$ by deriving $\log(\mathcal{L}_0)$ with respect to $\mathbf{\Phi}^{-1}$. This involves by deriving the trace of $(\mathbf{x}_k^{tH}\mathbf{T}_k^{-1})\mathbf{\Phi}^{-1}(\mathbf{T}_k^{-1}\mathbf{x}_k^t)$ with respect to $\mathbf{\Phi}^{-1}$ (see Eq. (101) in [**?**]):

$$\frac{\partial \log(\mathcal{L}_0)}{\partial \mathbf{\Phi}^{-1}} = 2N\mathbf{\Phi} - \sum_{\substack{k=1\\t=1}}^{\substack{k=N\\t=2}} \mathbf{T}_k^{-1}\mathbf{x}_k^t\mathbf{x}_k^{tH}\mathbf{T}_k^{-1} = \mathbf{0}_{mp}\,.$$

We finally obtain: $\hat{\mathbf{\Phi}} = \frac{1}{2N}\sum_{\substack{k=1\\t=1}}^{\substack{k=N\\t=2}} \hat{\mathbf{T}}_k^{-1}\mathbf{x}_k^t\mathbf{x}_k^{tH}\hat{\mathbf{T}}_k^{-1}$.

Appendix

The same approach is used for H_1: the texture parameters and the covariance parameter are optimized separately:

$$\log(\mathcal{L}_1) = C - \sum_{\substack{k=1\\t=1}}^{\substack{k=N\\t=2}} \log\left(|\boldsymbol{\Phi}_t|\right) + 2\sum_{\substack{k=1\\t=1}}^{\substack{k=N\\t=2}} \log\left(\left|\left(\mathbf{T}_k^t\right)^{-1}\right|\right) - \sum_{\substack{k=1\\t=1}}^{\substack{k=N\\t=2}} \left(\mathbf{x}_k^{tH}\left(\mathbf{T}_k^t\right)^{-1}\boldsymbol{\Phi}_t^{-1}\left(\mathbf{T}_k^t\right)^{-1}\mathbf{x}_k^t\right).$$

Appendix

Similarly to H_0, let us derive $\log(\mathcal{L}_1)$ with respect to $(\mathbf{T}_k^t)^{-1}$ and $\mathbf{\Phi}_t^{-1}$:

$$\frac{\partial \log(\mathcal{L}_1)}{\partial \left(\mathbf{T}_k^t\right)^{-1}} = 2 \sum_{\substack{k=1\\t=1}}^{\substack{k=N\\t=2}} \mathbf{T}_k^t - 2 \sum_{\substack{k=1\\t=1}}^{\substack{k=N\\t=2}} \operatorname{Re}\left(\mathbf{\Phi}_t^{-1} \left(\mathbf{T}_k^t\right)^{-1} \mathbf{x}_k^t \mathbf{x}_k^{tH}\right),$$

$$\frac{\partial \log(\mathcal{L}_1)}{\partial \mathbf{\Phi}_t^{-1}} = \sum_{\substack{k=1\\t=1}}^{\substack{k=N\\t=2}} \mathbf{\Phi}_t - \sum_{\substack{k=1\\t=1}}^{\substack{k=N\\t=2}} \mathbf{T}_{tk}^{-1} \mathbf{x}_k^t \mathbf{x}_k^{tH} \mathbf{T}_{tk}^{-1},$$

Letting the two previous equations be equal to $\mathbf{0}_{m\,p}$ leads to the following joint fixed point equations:

$$\begin{cases} \hat{\mathbf{T}}_k^t = \operatorname{Re}\left(\hat{\mathbf{\Phi}}_t^{-1} \left(\hat{\mathbf{T}}_k^t\right)^{-1} \mathbf{x}_k^t \mathbf{x}_k^{tH}\right), \\ \hat{\mathbf{\Phi}}_t = \frac{1}{N} \sum_{k=1}^{k=N} \left(\hat{\mathbf{T}}_k^t\right)^{-1} \mathbf{x}_k^t \mathbf{x}_k^{tH} \left(\hat{\mathbf{T}}_k^t\right)^{-1}. \end{cases} \quad (1)$$

Appendix

Multiband SAR modeling - Closed-form Solution (two-band case only)

Under H_0, we have

$$\hat{\mathbf{T}}_k = \begin{pmatrix} \hat{\delta}_{1_k} & 0 \\ 0 & \hat{\delta}_{2_k} \end{pmatrix} ,$$

with

$$\begin{cases} \hat{\delta}^2_{1_k} = \dfrac{1}{2} \displaystyle\sum_{t=1}^{t=2} \left(a_1 + \sqrt{\dfrac{a_1}{a_2}} a_{12} \right) , \\ \hat{\delta}^2_{2_k} = \dfrac{1}{2} \displaystyle\sum_{t=1}^{t=2} \left(\sqrt{\dfrac{a_2}{a_1}} a_{12} + a_2 \right) . \end{cases}$$

and

$$a_1 = \frac{1}{p} \mathbf{x}^{tH}_{1,k} \left(\mathbf{M}^{-1} \right)_{11} \mathbf{x}^t_{1,k}, \, a_2 = \frac{1}{p} \mathbf{x}^{tH}_{2,k} \left(\mathbf{M}^{-1} \right)_{22} \mathbf{x}^t_{2,k}, \, a_{12} = \frac{1}{p} \mathrm{Re} \left(\mathbf{x}^{tH}_{1,k} \left(\mathbf{M}^{-1} \right)_{12} \mathbf{x}^t_{2,k} \right) .$$

Appendix

Multiband SAR modeling - Closed-form Solution (two-band case only)

Under H_1, we have:

$$\hat{\mathbf{T}}_{tk} = \begin{pmatrix} \hat{\delta}^t_{1_k} & 0 \\ 0 & \hat{\delta}^t_{2_k} \end{pmatrix} ,$$

with

$$\begin{cases} \left(\hat{\delta}^t_{1_k}\right)^2 = \hat{\tau}^t_{1_k} = a_1 + \sqrt{\dfrac{a_1}{a_2}} a_{12} , \\ \left(\hat{\delta}^t_{2_k}\right)^2 = \hat{\tau}^t_{2_k} = a_2 + \sqrt{\dfrac{a_2}{a_1}} a_{12} , \end{cases}$$

and

$$a_1 = \frac{1}{p} \mathbf{x}^{tH}_{1,k} \left(\mathbf{M}_t^{-1}\right)_{11} \mathbf{x}^t_{1,k}, \, a_2 = \frac{1}{p} \mathbf{x}^{tH}_{2,k} \left(\mathbf{M}_t^{-1}\right)_{22} \mathbf{x}^t_{2,k}, \, a_{12} = \frac{1}{p} \operatorname{Re}\left(\mathbf{x}^{tH}_{1,k} \left(\mathbf{M}_t^{-1}\right)_{12} \mathbf{x}^t_{2,k}\right) .$$

Appendix

Please note that, $\forall t \in \{1,2\}$ and both hypotheses, $\mathbf{x}^{tH}\hat{\mathbf{T}}_t^{-1}\hat{\boldsymbol{\Phi}}_t^{-1}\hat{\mathbf{T}}_t^{-1}\mathbf{x}^t$ is a positive real scalar:

$$\begin{aligned}
\mathbf{x}^{tH}\left(\hat{\mathbf{T}}_t\hat{\boldsymbol{\Phi}}_t\hat{\mathbf{T}}_t\right)^{-1}\mathbf{x}^t &= \mathrm{Re}\left(\mathrm{tr}\left(\left(\hat{\mathbf{T}}_t\hat{\boldsymbol{\Phi}}_t\hat{\mathbf{T}}_t\right)^{-1}\mathbf{x}^t\mathbf{x}^{tH}\right)\right), \\
&= \mathrm{tr}\left(\hat{\mathbf{T}}_t^{-1}\mathrm{Re}\left(\hat{\boldsymbol{\Phi}}_t^{-1}\hat{\mathbf{T}}_t^{-1}\mathbf{x}^t\mathbf{x}^{tH}\right)\right), \\
&= m\,p\,.
\end{aligned}$$

Plugging the estimated parameters leads to the statistic $\hat{\Lambda}_B(\mathbf{x})$.

Appendix

- Illustration of models on real data [1].

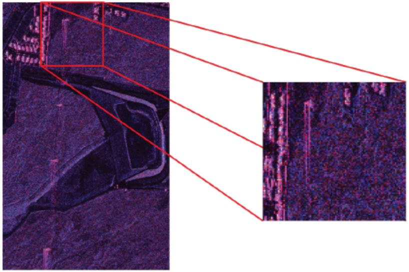

High-Resolution SAR image (Left) and a selected subset (Right) for HH polarization.

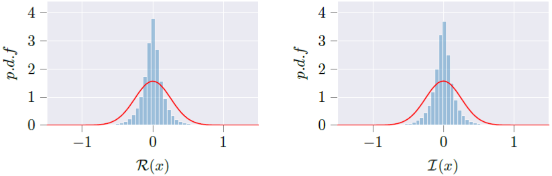

Gaussian fitting on the selected subset.

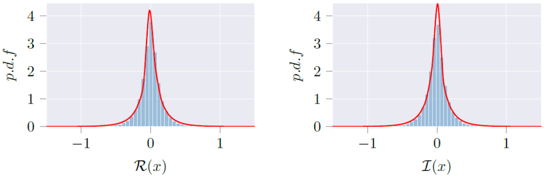

Textured Gaussian fitting on the selected subset